

## NUMERICAL SIMULATION ON AN AIRFOIL PLACED IN A UNIFORM VELOCITY FIELD

### *The problem*

In the year of 1983, A. Nakayama conducted several experiments in the aerodynamic tunnel on a conventional airfoil, designated name “model\_a”, at zero incidence [11]. He followed the determination of pressure coefficients distributions over the profile lateral surface, velocity distributions in the boundary layer and flow characteristics in the wake (using wire anemometry). The Reynolds number attached to the flow, computed with the chord length ( $c=610$  mm) was equal to  $Re=1.2\dot{1}10^6$  (the mean velocity in the wind tunnel was  $u=30.5$  m/s). In Figure 1 is represented the profile “model\_a”, as it is stored in the *European Research Community on Flow, Turbulence and Combustion* (ERCOFTAC) Database Classic Collection.



Fig. 1. Conventional airfoil, designated code “model\_a”, that was used in the experiments of Nakayama [11]

The work that is described in this paper aimed to set up a numerical method to be used in studies regarding the airfoils aerodynamics. The experimental data that exists due to Nakayama’s experiments were used to validate the numerical method. For the computational process we used the commercial expert software FLUENT v. 6.23. The grid was generated using the software GAMBIT v.2.4.6. The results were postprocessed in TECPLOT 360 2009 and FLUENT v. 6.23.

### *The fluid domain*

The airfoil was placed in a circular fluid domain, with a diameter of 11 m. The distance between the leading edge and the inlet section and respectively between the trailing edge and the outlet section, measured along the  $Ox$  axis, is equal to 5 airfoil chords, assuring in that manner the existence of a section placed at a sufficient distance upstream the aerodynamic profile, in order to report the values of different parameters in respect to it. Additionally, the consistence of the numerical simulation results is assured and also, its independence relative to the geometrical conditions.

The circle that surrounds the fluid domain was divided in two equal parts, one of the circular arcs representing the inlet frontier, and the second one, the outlet frontier. That solution was chosen in order to avoid the using of solid boundaries at the edge of the domain that could debase the numerical solution, as a result of the discarding of the theoretically infinite fluid domain condition.

The simulation was effected considering a reference system attached to the model. The  $Ox$  axis is aligned to the profile chord.

The fluid domain was meshed using an unstructured grid, made from almost 400000 quad cells. The boundary layer zone had a special treatment. Here, the grid was adequately thickened in order to detect correctly the strong variations of the flow parameters. Hereby, the boundary layer zone was discretized in 20 layers, with a minimum characteristic dimension along the normal to solid surfaces of  $10^{-4}$  and a growth factor of 1%. Consequently, the number of the cells attached to the boundary layer zone is approximately equal to 40000, i.e. 10% of the total number of cells (Figure 3).

Starting from the frontier of the boundary layer throughout the exterior boundaries of the domain, the grid has a size function attached with a growth factor of 1%, starting from a minimum characteristic length of 1 mm (near the solid surfaces) and ending to a maximum one of 10 mm (near the exterior of the fluid domain).

Regarding the grid quality, it may be considered that is almost excellent. As it may be observed fin Figure 2, 90% of the total number of cells are beneath the value of 0.2 for the *EquiAngle Skew* parameter, and 99 % are beneath 0.4 for the same parameter.

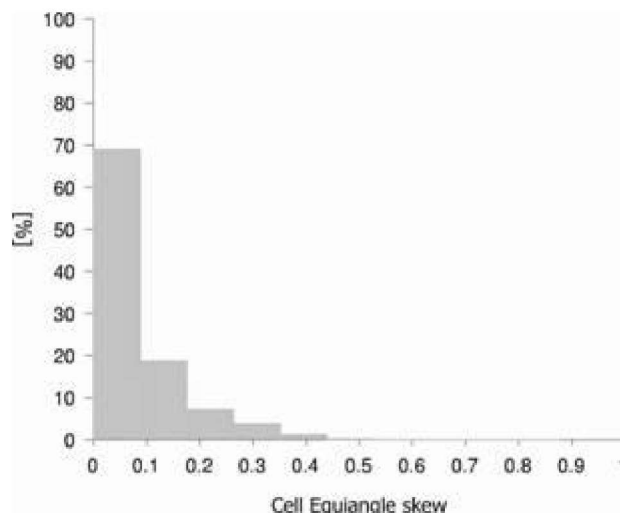


Fig. 2. EquiAngle Skew histogram repartition for the present case

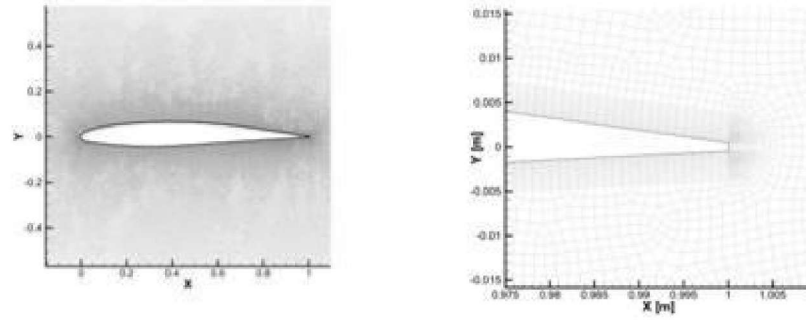


Fig. 3. Grid detail

#### Boundary conditions

The inlet of the fluid domain is made trough that frontier determined by the circular arc with a radius of 5.5 profile chords, subtending an angle of  $180^\circ$ , placed at a distance measured along  $Ox$  axis, equal with 5 profile chords, in respect to the leading edge. The velocity distribution is constant along the  $Oy$  axis, with a magnitude of 17.53 m/s, corresponding to a Reynolds number equal to  $1.2 \cdot 10^6$ .

The outlet of the domain is materialized by the second circular arc with a radius of 5.5 profile chords, which is subtending an angle of  $180^\circ$ . This is placed at a distance, measured along  $Ox$  axis, equal to 5 profile chords, in respect to the trailing edge of the airfoil. On the entire outlet frontier the pressure is equal to 0 on gage scale.

The curves that materialize the upper and lower surface of the aerodynamic profile have a no slip condition and they are rigid frontiers that do not permit mass or energy transfer.

#### Numerical model

Because of the fact that the phenomenon is developed at velocities that implies a high Reynolds number, the flow regime is turbulent. In order to describe correctly the fluid motion, it must be taken into account the viscosity effects. An inviscid solver is out of discussion. An LES solver is too much computational expensive. The most advanced RANS model implemented in FLUENT is RSM (Reynolds Stress Model). It offers a detailed description of the flow using the Reynolds Averaged Navier-Stokes equations.

In opposition to the isotropy of the turbulent viscosity hypothesis and its description using the Boussinesq linear approximation, the RSM model solves all the Reynolds stresses, adding seven additional equations for a 3D simulation and five for a 2D one. The RANS system, written in a Cartesian coordinate system, for an incompressible fluid, is written as follows:

$$\begin{aligned} \frac{\partial \bar{u}}{\partial x} + \frac{\partial \bar{v}}{\partial y} + \frac{\partial \bar{w}}{\partial z} &= 0 \\ \frac{D\bar{u}}{dt} &= f_x - \frac{1}{\rho} \frac{\partial \bar{p}}{\partial x} + \nu \left( \frac{\partial^2 \bar{u}}{\partial x^2} + \frac{\partial^2 \bar{u}}{\partial y^2} + \frac{\partial^2 \bar{u}}{\partial z^2} \right) + \frac{1}{\rho} \left[ \frac{\partial (-\rho \overline{u'u'})}{\partial x} + \frac{\partial (-\rho \overline{u'v'})}{\partial y} + \frac{\partial (-\rho \overline{u'w'})}{\partial z} \right] \\ \frac{D\bar{v}}{dt} &= f_y - \frac{1}{\rho} \frac{\partial \bar{p}}{\partial y} + \nu \left( \frac{\partial^2 \bar{v}}{\partial x^2} + \frac{\partial^2 \bar{v}}{\partial y^2} + \frac{\partial^2 \bar{v}}{\partial z^2} \right) + \frac{1}{\rho} \left[ \frac{\partial (-\rho \overline{v'u'})}{\partial x} + \frac{\partial (-\rho \overline{v'v'})}{\partial y} + \frac{\partial (-\rho \overline{v'w'})}{\partial z} \right] \\ \frac{D\bar{w}}{dt} &= f_z - \frac{1}{\rho} \frac{\partial \bar{p}}{\partial z} + \nu \left( \frac{\partial^2 \bar{w}}{\partial x^2} + \frac{\partial^2 \bar{w}}{\partial y^2} + \frac{\partial^2 \bar{w}}{\partial z^2} \right) + \frac{1}{\rho} \left[ \frac{\partial (-\rho \overline{w'u'})}{\partial x} + \frac{\partial (-\rho \overline{w'v'})}{\partial y} + \frac{\partial (-\rho \overline{w'w'})}{\partial z} \right] \end{aligned}$$

where  $\bar{u}$ ,  $\bar{v}$ ,  $\bar{w}$  are mean values of the velocity along  $Ox$ ,  $Oy$  and  $Oz$  axis,  $u'$ ,  $v'$ ,  $w'$  are velocity pulsations,  $\bar{p}$  is the mean pressure, and  $\nu$  is the kinematical viscosity of the fluid.

In order to solve the closure problem, is necessary to add another transport equation, used to describe the dissipation rate of the turbulent kinetic energy, similar to that utilized in a  $k-\epsilon$  turbulence model.

The solver selected for the computational process was a double precision pressure based one (pressure based solver). In order to discretize the continuity, momentum and turbulence model specific equations, 2<sup>nd</sup> order discretization schemes were used.

In the table no.1 are presented, synthetically, the computational parameters used for simulation.

Table 1

Parameter name	Parameter used
Model	2D
Turbulence model	RSM
Time	steady
Solver	pressure based

Discretization schemes	2 <sup>nd</sup> order
Precision	double precision

### Results

In order to validate the numerical method, we aimed to compute the values for the pressure coefficient  $C_p$  on the upper part and lower part of the airfoil, and also, velocity distribution in the boundary layer of the upper part, near the trailing edge. Those were compared to the experimental data available.

The pressure coefficient  $C_p$  is computed using the following relation:

$$C_p = \frac{P - P_\infty}{\frac{\rho u_\infty^2}{2}}$$

where  $p$  represents the value of the static pressure corresponding to a certain point placed on the airfoil surface,  $P_\infty$  the value of the static pressure, upstream, in the inlet section,  $\rho$  the density of the fluid and  $u_\infty$  the velocity of the fluid in the inlet section.

In Figure 5 are represented the pressure coefficient variation on the upper part and lower part of the airfoil, for numerical and experimental data.

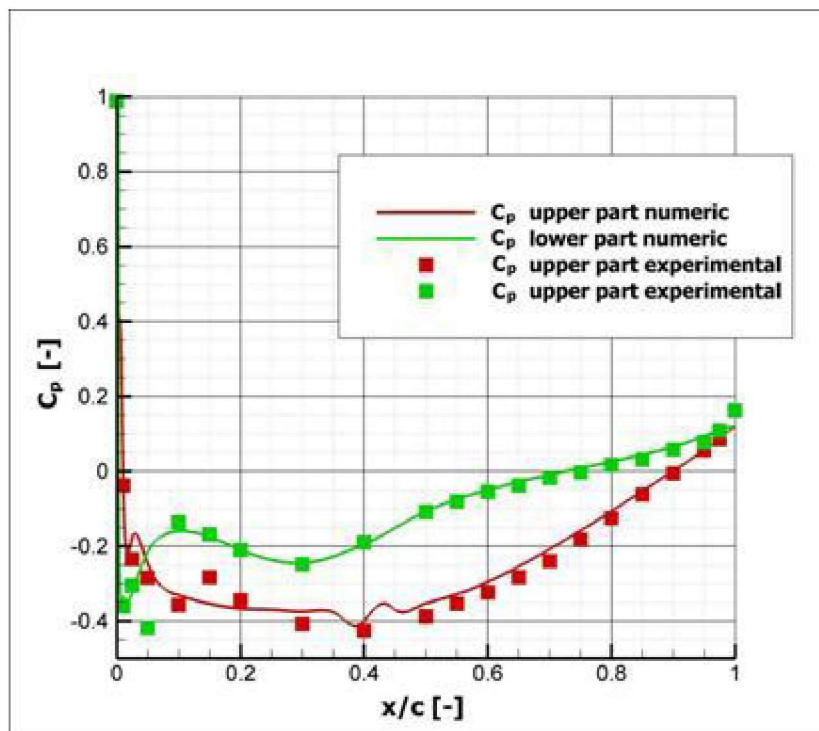


Fig. 5. Pressure coefficient  $C_p$  variation in respect with nondimensionalized distance  $x/c$  for the „model\_a” airfoil

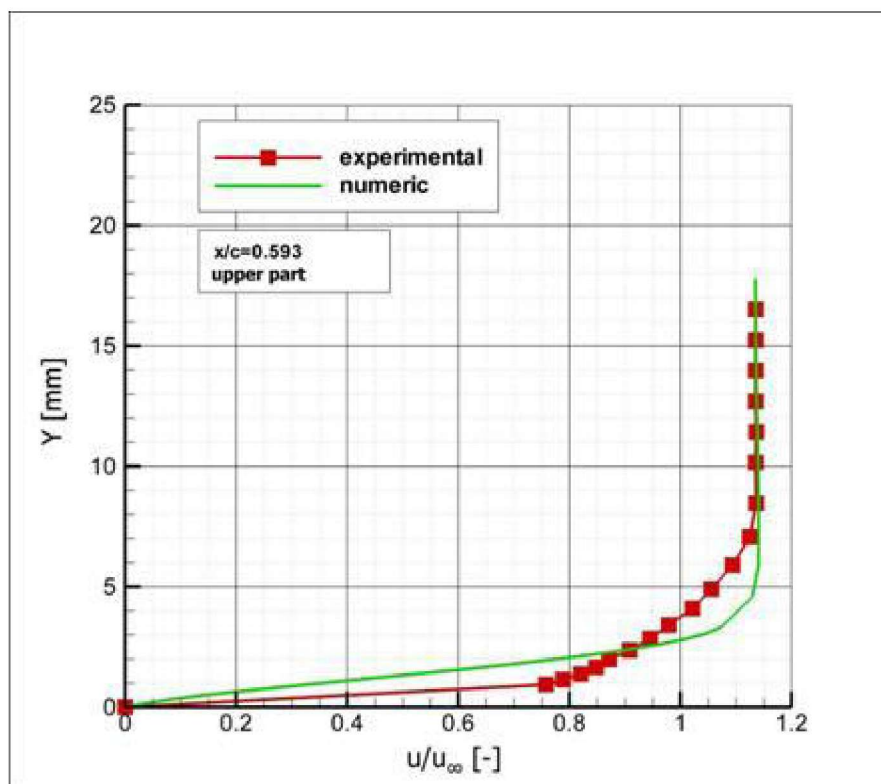


Fig. 6. Nondimensionalized velocity distribution  $u/u_{\infty}$  on the upper part of the „model\_a” airfoil for  $x/c=0.593$

In Figures 6 to 10 are represented the velocity profiles (computed numerically and determined experimentally) for five sections placed at distances  $x/c$  equals to 0.593, 0.893, 0.940, 0.970 and respectively 1. The velocity is nondimensionalized in respect to the velocity in the inlet section ( $u/u_{\infty}$ ).

The numerical results are validated with a sufficient accuracy by the data obtained in the aerodynamic tunnel experiments, for the pressure coefficient distribution but also for the kinematical ones. The errors are in normal limits, no more than 5%.

#### Conclusions

We tried to set up a numerical method to be used in studies regarding the airfoils aerodynamics. In order to do that, a RANS approach was chosen, using for that the most advanced turbulence model, i.e. RSM. The solver was a double precision pressure based coupled one and the discretization schemes used were of 2<sup>nd</sup> order.

The numerical results are validated by the data obtained in the aerodynamic tunnel experiments. The errors are in normal limits, no more than 5%. We may observe that, for the velocity distribution, in the boundary layer, near the wall (0...5 mm), the numerical model gives the largest errors. That may be caused by the fact that the precision of the RSM model is still limited by the closure problem (a 2<sup>nd</sup> order one), which may be solved more or less correctly, in respect to the hypothesis used for modeling different additional terms in transport equations for Reynolds efforts.

The method may be used in numerical studies regarding the airfoils aerodynamics.

**Bibliography:** 1. ANSYS, INC., „FLUENT 6.3 User’s Guide”, 2006. 2. ANSYS, INC., „GAMBIT 2.4 User’s Guide”, 2007. 3. BALINT D.I., „Metode numerice de calcul al câmpurilor tridimensionale în distribuitorul și rotorul turbinei Kaplan”, Teză de doctorat, Universitatea „Politehnica” din Timișoara, România, 2008. 4. BENJANIRAT S., SANKAR L.N., „Evaluation of turbulence models for the prediction of wind turbine aerodynamics”, 41st Aerospace Sciences Meeting and Exhibit, Reno, Nevada, Jan. 6-9, 2003. 5. BERNAD, I.S., „Hidrodinamica echipamentelor de reglare pentru acționări hidraulice”, Editura Orizonturi Universitare, Timișoara, 2005. 6. BERNAD S.I., BĂRBAT T., GEORGESCU A.M., GEORGESCU S.M., SUSAN-RESIGA R. „Unsteady Flow Simulation in the Achard Turbines Mounted in Hydropower Farms”, Scientific Bulletin of the Politehnica University of Timișoara, Transactions on Mechanics Tom 53 (67), 2008. 7. COȘOIU C.I. „Contribuții la optimizarea proiectării și funcționării agregatelor eoliene”, PhD thesis, 2008. 8. COȘOIU C.I. Grant PN II TD-242, „Contribuții la optimizarea proiectării și funcționării agregatelor eoliene”, Research Raport, 2007. 9. FERZIGER J., PERIC M., „Computational Methods for Fluid Dynamics”, Springer, 1996. 10. GEORGESCU A.M., GEORGESCU C.S., DEGERATU M., BERNADS, COȘOIU, C.I., „Numerical modelling comparison between air flow and water flow within achard-type turbine”, Proceeding of the 2nd IAHR international meeting of the workgroup on cavitation and dynamic problems in hydraulic machinery and systems, Timișoara, România, October 2007. 11. NAKAYAMA A. „Characteristics of the flow around conventional and supercritical airfoils”, Journal of Fluid Mechanics, 160, 155, 1985. 12. PRANDTL L. „Über die Entstehung von Wirbeln in der idealen Flüssigkeit, mit Anwendung auf die Tragflügeltheorie und andere Aufgaben”, In: von Kármán and Levi-Cevita, Editors, Vorträge aus dem Gebiete der Hydro und Aerodynamik, Springer, Berlin (1922).